BIOCHEMISTRY
including biophysical chemistry & molecular biology

Article

pubs.acs.org/biochemistry

Mechanism of Inhibition for N6022, a First-in-Class Drug Targeting *S*-Nitrosoglutathione Reductase

Louis S. Green,[†] Lawrence E. Chun,[‡] Aaron K. Patton,[†] Xicheng Sun,[†] Gary J. Rosenthal,[†] and Jane P. Richards*[,†]

[†]N30 Pharmaceuticals, LLC, 3122 Sterling Circle, Suite 200, Boulder, Colorado 80301, United States

[‡]Emerald BioStructures, 7869 Northeast Day Road West, Bainbridge Island, Washington 98110, United States

Supporting Information

ABSTRACT: N6022 is a novel, first-in-class drug with potent inhibitory activity against *S*-nitrosoglutathione reductase (GSNOR), an enzyme important in the metabolism of *S*-nitrosoglutathione (GSNO) and in the maintenance of nitric oxide (NO) homeostasis. Inhibition of GSNOR by N6022 and related compounds has shown safety and efficacy in animal models of asthma, chronic obstructive pulmonary disease, and inflammatory bowel disease [Sun, X., et al. (2011) *ACS Med. Chem. Lett.* 2, 402−406]. N6022 is currently in early phase clinical studies in humans. We show here that N6022 is a tight-binding, specific, and fully reversible inhibitor of GSNOR with an IC_{50} of 8 nM and a K_i of 2.5 nM. We accounted for the fact that the NAD^+- and NADH-dependent oxidation and reduction reactions, catalyzed by GSNOR are bisubstrate in nature in our calculations. N6022 binds in the GSNO substrate binding pocket like a competitive inhibitor, although in kinetic assays it behaves with a mixed uncompetitive mode of inhibition (MOI) toward the GSNO substrate and a mixed competitive MOI toward the formaldehyde adduct, *S*-hydroxymethylglutathione (HMGSH). N6022 is uncompetitive with cofactors NAD^+ and NADH. The potency, specificity, and MOI of related GSNOR inhibitor compounds are also reported.

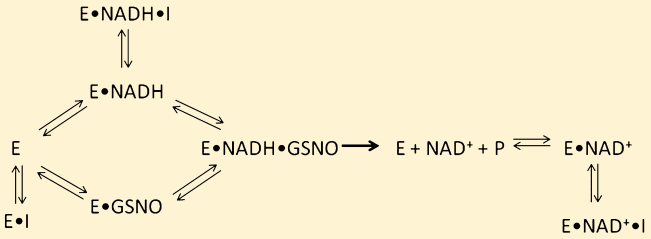

GSNOR is a zinc-dependent, NAD^+- and NADH-dependent, medium chain alcohol dehydrogenase (ADH) that plays an important role in nitrosative biology by metabolizing the *S*-nitrosothiol, GSNO. Human GSNOR is the same enzyme as ADH class III (ADH III), also known as the ADH-χ subunit in earlier literature. Unlike the other ADH enzymes, GSNOR has poor activity against ethanol, although it is modestly active against hydrophobic, long chain primary alcohols and aldehydes, particularly the ω-hydroxy fatty acids.[1,2] GSNOR is also known as formaldehyde dehydrogenase (FDH) and plays a role in formaldehyde detoxification.[3−5] Formaldehyde metabolism by GSNOR requires the presence of GSH, which spontaneously reacts with formaldehyde to form *S*-hydroxymethylglutathione (HMGSH), an efficient substrate for the enzyme. HMGSH and GSNO are both glutathione adducts differing only in the functional group attached to the single sulfur atom. GSNOR is highly conserved among bacteria, plants, yeast, and animals and is thought to be the ancestral ADH from which all other ADH enzymes evolved by gene duplication.[6−8] In mammals, GSNOR is widely distributed across all tissue and organ systems,[9−11] although cell-type specific expression within tissues has been noted.[12]

Jensen et al. first discovered that GSNO was a highly efficient substrate for the rat ADH III/FDH/GSNOR enzyme and proposed that metabolism of GSNO by the enzyme played a physiological role in NO exchange equilibrium and the signal transduction processes that lead to protein S-nitrosation.[13] With a catalytic efficiency, k_{cat}/K_m, on the order of 1.9×10^6 M^{-1} s^{-1}, the reduction of GSNO by GSNOR is the most efficient reaction of any of the ADH enzymes characterized so far. By comparison, the metabolically important ethanol oxidation reactions of the human liver ADH I enzymes have k_{cat}/K_m values on the order of only 100−1000 M^{-1} s^{-1}.[7] The importance of GSNOR in controlling levels of both intracellular GSNO and nitrosated proteins was soon confirmed in knockout models of yeast and mice, and the nomenclature "GSNO reductase" was introduced to reflect this important physiological role.[14] The significance of GSNOR in GSNO metabolism and nitrosative biology in both normal and pathophysiological states has been highlighted in recent reviews.[15−17]

GSNOR is a homodimeric enzyme with no evidence of cooperativity between the subunits, and several crystal structures of the enzyme have been published.[18−21] Each monomeric subunit consists of a large catalytic domain comprised of the N-terminal half of the protein and a C-terminal cofactor binding domain that makes up much of the subunit dimerization interface. The active site lies in a large cleft between the cofactor and catalytic domains. There are two zinc molecules per subunit, both in the catalytic domain: one zinc atom forms part of the active site and is essential for catalysis, and the other zinc serves a purely structural function. The reaction mechanism is generally thought to be random order

Received: December 2, 2011
Revised: February 14, 2012
Published: February 15, 2012

   dx.doi.org/10.1021/bi201785u | *Biochemistry* 2012, 51, 2157−2168

bi-bi,[22] but this has not been specifically reported for the GSNO substrate.

Electrospray mass spectrometry identified glutathione sulfinamide as the major reaction product of GSNO reduction by GSNOR[23] (Supporting Information). The immediate reaction product is the unstable intermediate semimercaptal, *S*-(*N*-hydroxylamino)glutathione, which spontaneously rearranges to form glutathione sulfinamide or, in the presence of GSH, forms oxidized glutathione (GSSG) and hydroxyl amine.[13,23−25] Under acidic conditions, the glutathione sulfinamide is easily hydrolyzed to glutathione sulfinic acid and ammonia.[13] The GSNO reduction reaction is irreversible, and glutathione sulfinamide, GSH, and GSSG are neither substrates nor inhibitors of GSNOR activity.[23,25] The irreversible nature of the GSNO reduction reaction is in contrast to the reversible oxidation of HMGSH by GSNOR and the mostly reversible alcohol/aldehyde oxido-reduction reactions catalyzed by the other ADH enzymes. The irreversible reduction of GSNO by GSNOR therefore removes GSNO from the NO-donating pool without the concomitant release of NO.[13,24,26]

Recent mechanistic and preclinical studies provide experimental support for GSNOR as a target for therapeutic intervention.[27,28] Inhibition of GSNOR prevents GSNO metabolism and allows accumulation of GSNO, which is a broncho- and vasodilator as well as an initiator of anti-inflammatory signaling.[29−31] An increased level of GSNO as a result of GSNOR inhibition leads to cellular signaling by direct protein S-nitrosation and is also thought to influence the levels of NO and nitrite (NO_2^-) that form via reactions of GSNO with glutathione (GSH) or various reactive oxygen or nitrogen species.[32,33] GSNOR inhibitors are being developed as a therapeutic strategy for treating conditions under which GSNO and NO homeostasis has been disrupted.[33−36] As a first indication, the GSNOR inhibitor N6022 is under clinical development for the treatment of inflammatory lung diseases. In this study, we examine the specificity, reversibility, and kinetic mode of inhibition of N6022 and related compounds as they interact with GSNOR. We calculated the inhibitor dissociation constant, K_i, using Cheng−Prusoff equations that relate the IC_{50} to K_i and that we further adapted to account for the bisubstrate nature of GSNOR and the tight-binding nature of these inhibitors.

MATERIALS AND METHODS

Materials. Highly pure, pharmaceutical grade GSNO was manufactured for N30 Pharmaceuticals under Good Manufacturing Practices by Ricerca Biosciences (Concord, OH). N6022 was synthesized at N30 Pharmaceuticals as previously described.[34] [^{14}C]N6022 (65 mCi/mmol) was prepared at Moravek Biochemicals (Brea, CA). Formaldehyde was purchased from Thermo Scientific. All other chemicals and reagents were purchased from either Sigma-Aldrich or VWR. Absorbance assays were performed using either a Molecular Devices Spectramax M2 plate reader or a Shimadzu UV−vis dual-beam spectrophotometer. All experiments were conducted at room temperature unless noted. Data analysis was performed using GraphPad Prism version 5.03.

Protein Purification. Full-length, recombinant human GSNOR, ADH IB, ADH II, ADH IV, and human carbonyl reductase 1 were produced in *Escherichia coli* as Smt fusion proteins containing an N-terminal histidine affinity tag. *E. coli* cell paste was lysed by nitrogen cavitation and the clarified lysate purified by Ni affinity chromatography on an AKTA FPLC system (Amersham Pharmacia). The column was eluted in 20 mM Tris (pH 8.0) and 250 mM NaCl with a 0 to 500 mM imidazole gradient. Eluted GSNOR, ADH IB, ADH II, ADH IV, and carbonyl reductase 1 fractions containing the His-Smt fusion tag were digested overnight with Ulp-1 at 4 °C to remove the affinity tag and then run again on the Ni column under the same conditions. Proteins were recovered in the flow-through fraction and further purified with Q-Sepharose and heparin flow-through chromatography (GE Healthcare columns) in 20 mM Tris (pH 8.0), 1 mM DTT, and 10 μM $ZnSO_4$. Purity was confirmed by sodium dodecyl sulfate−polyacrylamide gel electrophoresis.

GSNOR Assays. GSNOR activity for the reduction of GSNO was determined by measuring the NADH- and GSNO-dependent decrease in absorbance at 340 nm (A_{340}) as previously described.[13] Progress curves were depicted as a decrease in absorbance over time due to NADH and GSNO consumption with a linear slope equal to the reaction velocity. Kinetic constants were determined at room temperature in 100 mM sodium phosphate buffer (pH 7.4) with a GSNOR concentration of 11 nM. For GSNO constants, NADH was at a fixed concentration of 300 μM while the GSNO concentration ranged from 0.5 to 240 μM. For the NADH constants, the GSNO concentration was fixed at 300 μM and the NADH concentration ranged from 0.6 to 300 μM. GSNOR activity for the oxidation of HMGSH by NAD^+ was determined by measuring the increase in A_{340} due to reduction of NAD^+ to NADH using conditions similar to those described previously.[22] An HMGSH stock solution was prepared by mixing methanol-free formaldehyde from sealed ampules and glutathione both to 30 mM in 100 mM sodium phosphate (pH 7.4). HMGSH concentrations for this stock solution and subsequent dilutions were calculated with a K_{eq} for adduct dissociation of 1.77 mM as previously described.[22] Kinetic constants were determined in 100 mM sodium phosphate buffer (pH 8.9) with a GSNOR concentration of 40 nM. For HMGSH constants, NAD^+ was at a fixed concentration of 300 μM while the HMGSH concentration ranged from 0.003 to 44 μM. For the NAD^+ constants, the HMGSH concentration was fixed at 83 μM and the NAD^+ concentration ranged from 0.4 to 200 μM. Kinetic constants for all reactions were determined from a plot of the initial linear reaction rate versus substrate concentration and fit to a Michaelis−Menten model.

To measure the IC_{50} of N6022 and related compounds against GSNOR, the compounds were first dissolved in DMSO. The final assay conditions for the GSNO reduction reaction were 100 mM sodium phosphate (pH 7.4), 240 μM GSNO, 300 μM NADH, 0.5 μg/mL GSNOR, and 1% DMSO. For the determination of the IC_{50} of the HMGSH oxidation reaction, the final assay conditions were 100 mM sodium phosphate (pH 8.9), 58 μM HMGSH, 300 μM NAD^+, 1.5 μg/mL GSNOR, and 1% DMSO.

ADH Enzyme Assays. For ADH IB, ADH II, and ADH IV assays, enzyme activity was determined by measuring the increase in A_{340} due to reduction of NAD^+ to NADH using conditions similar to those described by Sanghani et al.[32] N6022 was dissolved and diluted in a PBS solution containing 1 N NaOH (1%). The IC_{50} values for N6022 versus ADH IB and ADH II were determined with ethanol as the substrate. The final assay conditions for ADH IB were 50 mM sodium phosphate (pH 7.4), 20 μg/mL ADH IB, 2 mM NAD^+, and 2 mM ethanol, and the final assay conditions for ADH II were 90 mM sodium pyrophosphate (pH 8.9), 4.4 μg/mL ADH II, 23.6 mM NAD^+, and 14.4 mM ethanol. The IC_{50} value of N6022 against ADH IV was determined using hexanol as a

substrate. The hexanol was first dissolved in DMSO so that it could be dissolved in assay buffer. The final assay conditions were 50 mM sodium phosphate (pH 7.4), 1.25 μg/mL ADH IV, 2 mM NAD^+, 400 μM hexanol, and 1% DMSO. Other inhibitors were either prepared in PBS containing 1 N NaOH (1%) (for ADH IB and ADH II) or dissolved in DMSO (for ADH IV and GSNOR). DMSO at 1% interfered with the enzyme activity of ADH IB and ADH II, but not that of ADH IV or GSNOR (not shown). The IC_{50} assays for additional inhibitors were performed as described for N6022 except for ADH IV, in which ethanol was used as a substrate with final assay conditions of 25 mM sodium pyrophosphate (pH 8.9), 2.5 μg/mL ADH IV, 7.5 mM NAD^+, 28 mM ethanol, and 1% DMSO.

Active Enzyme Concentration. The purified enzyme concentration was determined spectrophotometrically at A_{280} using a calculated extinction coefficient of 33305 M^{-1} cm^{-1} based on amino acid sequence. Standard assays contained 0.5 μg/mL GSNOR (equal to 12.6 nM GSNOR monomer with a calculated molecular weight of 39593). Because even the highly purified enzyme may not contain 100% active protein, the amount of active GSNOR was determined by a method described by Copeland, where IC_{50} is plotted as a function of apparent enzyme concentration under conditions where the $K_i^{app}/[E]_t$ ratio falls between 10 and 0.01.[37] The IC_{50} values were determined at seven GSNOR concentrations with 11 inhibitor dilutions. The IC_{50} versus GSNOR concentration was plotted and fit by linear regression (not shown). By this method, twice the slope (m) of the linear fit yields the fraction of the apparent enzyme concentration that is active per the equation $[E]_t = 2m[E]^{app}$. The active GSNOR concentration was determined to be approximately 86% of the enzyme concentration measured by absorbance or 11 nM GSNOR monomer.

Dilution and Recovery Assay. GSNOR at 10 μg/mL was preincubated with 100 nM N6022 (approximately 10-fold above the IC_{50}) in 100 mM phosphate buffer (pH 7.4) for 10, 20, or 30 min at 25 °C. The GSNOR/inhibitor mixtures were then diluted 100-fold directly into a substrate mixture to give final assay conditions of 0.1 μg/mL GSNOR, 1 nM N6022, 240 μM GSNO, and 300 μM NADH in 100 mM phosphate buffer (pH 7.4). The GSNOR enzyme activity was determined immediately after dilution by following the change in A_{340} for 5 min. Under these conditions, theoretical recovery of a fully reversible inhibitor is 91%, because an inhibitor at one-tenth of the IC_{50} concentration remains in the diluted reaction. Control reactions were performed under the same conditions as the diluted assay, but without preincubation and dilution. Recovery was determined as percent activity of a reaction performed under the same conditions without inhibitor.

Mode of Inhibition. The inhibitor MOI was determined for each substrate separately (i.e., substrate and cofactor), where the concentration of one substrate was varied while that of its cosubstrate was held at a fixed, saturating concentration. Inhibitors were prepared in DSMO. The final conditions for the GSNO reduction reaction were 0.5 μg/mL GSNOR, 240 μM (or varied) GSNO, 300 μM (or varied) NADH, 100 mM sodium phosphate buffer (pH 7.4), 1% DMSO, and inhibitor. The final conditions for the HMGSH oxidation assays were 1.5 μg/mL GSNOR, 58 μM (or varied) HMGSH, 300 μM (or varied) NAD^+, 100 mM sodium phosphate (pH 8.9), 1% DMSO, and inhibitor. IC_{50} values were determined from 11 concentrations of inhibitor at each of eight concentrations of the varied substrate. A plot of IC_{50} versus substrate concentration was made, and the data were fit to the appropriate Cheng–Prusoff equation (eq 1). Scheme 1 describes the nomenclature we used in our equations.

Scheme 1. Simplified Reaction Scheme Illustrating the Assignment of K_{i1} and K_{i2}[a]

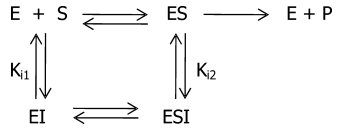

[a]For the GSNOR reaction, the second substrate was held constant at a saturating concentration and is not depicted in the schematic. The reduction of GSNO by GSNOR and NADH is irreversible (pictured), whereas the oxidation of HMGSH by GSNOR and NAD^+ is reversible (not pictured). Abbreviations: E, enzyme; S, substrate; I, inhibitor; P, product.

Equation 1, from Copeland,[37] was used to fit the IC_{50} as a function of substrate concentration data presented in Figure 3 and to solve for K_{i1}, K_{i2}, and K_m using user-defined equations in GraphPad Prism. Because N6022 was determined to be a tight-binding inhibitor (see Results), we followed the approach described by Copeland and included a term to account for total enzyme concentration. The term, $^1/_2[E]_t$, represents the limiting enzyme concentration that allows 50% of inhibitor to be bound and is therefore the lowest IC_{50} that can be measured. The constant α was determined from the relationship $\alpha = K_{i2}/K_{i1}$, and we assigned a MOI for the inhibitor against each substrate according to the α value.[38] We categorized the MOI as competitive ($\alpha \geq 100$), mixed competitive ($100 > \alpha > 1$), noncompetitive ($\alpha = 1$), mixed uncompetitive ($1 > \alpha > 0.01$), or uncompetitive ($\alpha \leq 0.01$) toward a given substrate. The concentration of active GSNOR enzyme ($[E]_t$) was fixed at 11 nM for the GSNO reaction and 33 nM for the HMGSH reaction, and the K_m for each substrate was not constrained. MOI data were also analyzed with the Morrison quadratic equations[39] that gave values for K_{i1}, K_{i2}, and α in good agreement with the Cheng–Prusoff analysis (not shown).

$$IC_{50} = \frac{[S] + K_m}{K_m/K_{i1} + [S]/K_{i2}} + \frac{1}{2}[E]_t \quad (1)$$

Equation 1 can be rearranged, ignoring the term for tight binding, and solved for either K_{i1} or K_{i2}. The results are eqs 2 and 3. The equation for K_{i1} is used to describe a mixed competitive inhibitor, and the equation for K_{i2} is used for a mixed uncompetitive inhibitor. Note for both eqs 2 and 3, if the MOI is either purely competitive or purely uncompetitive, the term $1 - IC_{50}/K_i$ in the denominator equals 1 and can be ignored.

$$K_{i1} = \frac{IC_{50}}{1 + [S]/K_m(1 - IC_{50}/K_{i2})} \quad (2)$$

$$K_{i2} = \frac{IC_{50}}{1 + K_m/[S](1 - IC_{50}/K_{i1})} \quad (3)$$

GSNOR is a bisubstrate enzyme, so neither K_{i1} nor K_{i2} in our experiment was measuring the true K_i of the inhibitor for the free enzyme, because there was always a saturating amount of one of the substrates present. Further calculation was necessary to determine the overall inhibitor dissociation constant, K_i, of N6022 for GSNOR. This calculation must account for the MOI

dx.doi.org/10.1021/bi201785u | Biochemistry 2012, 51, 2157–2168

with respect to each substrate in the reaction, as well as the concentration of each substrate in the IC_{50} assay and the K_m of each substrate. Therefore, to determine the final K_i of the inhibitor and GSNOR, we took the product of the terms for each of the two substrates.[40]

We used eq 4 to calculate the K_i from the IC_{50} data of the GSNO reduction reaction. Equation 4 accounts for the purely uncompetitive relationship of N6022 with NADH ($1 + K_m^{NADH}$/NADH) and the mixed uncompetitive relationship of N6022 with GSNO (term in braces in the denominator). We used eq 5 to calculate the K_i from IC_{50} data of the HMGSH oxidation reaction. Equation 5 accounts for the mixed uncompetitive relationship of N6022 against NAD^+ (first term in braces in the denominator) and the mixed competitive relationship of N6022 against HMGSH (second term in braces in the denominator). For tight-binding inhibitors, the active enzyme concentration was accounted for by subtracting [E]/2 from the IC_{50} value.[37] In our calculations, the K_m value used for each substrate was the value that resulted from the fit of the IC_{50} versus substrate concentration data to eq 1.

$$K_i = \left(IC_{50} - \frac{[E]_t}{2}\right) \Bigg/ \left((1 + K_m^{NADH}/[NADH]) \left\{ 1 + (K_m^{GSNO}/[GSNO]) \left[1 - \left(IC_{50} - \frac{[E]_t}{2} \right) / K_{i1}^{GSNO} \right] \right\} \right) \quad (4)$$

$$K_i = \left(IC_{50} - \frac{[E]_t}{2}\right) \Bigg/ \left(\left\{ 1 + (K_m^{NAD}/[NAD]) \left[1 - \left(IC_{50} - \frac{[E]_t}{2} \right) / K_{i1}^{NAD} \right] \right\} \left\{ 1 + ([HMGSH]/K_m^{HMGSH}) \left[1 - \left(IC_{50} - \frac{[E]_t}{2} \right) / K_{i2}^{HMGSH} \right] \right\} \right) \quad (5)$$

[^{14}C]N6022 Filter Binding Assay. For the competition of GSNO with the [^{14}C]N6022·GSNOR·NAD^+ ternary complex, a mixture of 33 nM [^{14}C]N6022, 330 nM GSNOR, and 50 μM NAD^+ in 100 mM Na_2HPO_4 (pH 8.9) was prepared. GSNO dilutions to give final concentrations of GSNO ranging from 50 nM to 3 mM were added to 1 mL aliquots of the mixture and allowed to equilibrate for 10 min. Each 1 mL aliquot was filtered through prewashed nitrocellulose filters on a vacuum manifold, followed by a 2 mL wash with buffer. The filters were briefly placed on absorbent paper to remove buffer that adhered to the back of the filters, moved to aluminum foil, and dried at 70 °C for 5 min in a convection oven. The dried filters were transferred to scintillation vials; 4 mL of scintillation fluid was added, and the counts per minute per vial were determined in a Beckman LS6500 liquid scintillation counter. Two additional filters were spotted with undiluted [^{14}C]N6022 equivalent to that in 1 mL aliquots of the competition mix, dried, and counted to determine the total counts per minute per well (~10000 or ~20000 cpm with 30 or 60 nM [^{14}C]N6022, respectively). For the HMGSH competition with the [^{14}C]N6022·GSNOR·NADH complex, a mixture of 50 nM [^{14}C]N6022, 360 nM GSNOR, and 50 μM NADH in 100 mM Na_2HPO_4 (pH 8.9) was prepared. HMGSH dilutions to give final concentrations ranging from 0.001 to 480 μM were added to 1 mL aliquots of the mix. Equilibration, filtration, washing, and counting were conducted as for the GSNO experiment. The dissociation constant for HMGSH was determined using the GraphPad Prism curve fitting software and a one-binding site model with ligand depletion, because the concentration of the enzyme was greater than the concentration of the radioligand. The K_d for N6022 and the GSNOR·NADH complex used in the calculation was the value of K_{i1} from Table 3. The ^{14}C was incorporated randomly into the benzene ring of N6022 with a low stoichiometry and should not affect the protein binding interaction.

Crystallization of GSNOR. Purified GSNOR was dialyzed against 20 mM Tris (pH 8.0), 50 mM NaCl, 1 mM DTT, and 10 μM $ZnSO_4$ at 4 °C and then concentrated to ~14 mg/mL for crystallization trials. For cocrystallization trials, N6022 and NAD^+ were added at 10- and 5-fold molar excesses, respectively, and incubated overnight at 4 °C prior to concentration. Apo-GSNOR and GSNOR·inhibitor complexes were crystallized in sitting drops by vapor diffusion in 19% PEG 8000, 0.1 M potassium phosphate (pH 7.0), 0.1 mM $ZnSO_4$, 1 mM DTT, and 3% (v/v) 1,5-diaminopentane *d*-HCl at 4 °C. The crystal structure of the N6022·GSNOR·NAD^+ ternary complex (Protein Data Bank entry 3QJ5) was determined to 1.9 Å by molecular replacement using 1MC5 as the search model.[33] The model contains one GSNOR dimer in the asymmetric unit with each monomer containing one inhibitor molecule, one coenzyme molecule, and two zinc atoms. Images were created using PyMOL.

RESULTS

GSNOR Reaction Kinetics. Purified, recombinant human GSNOR was used for all experiments. Two reactions were studied to characterize the inhibitor mechanism of N6022: the reduction of GSNO by NADH and the oxidation of the formaldehyde adduct, HMGSH, by NAD^+ (see the Supporting Information). The kinetic constants obtained in our system are listed in Table 1. Our values generally agree with those published previously (ref 26 and references therein).

Activity of N6022 against Other Enzymes of the ADH Family. N6022 is a pyrrole-based, small molecule inhibitor of GSNOR and represents a novel class of compounds designed for therapeutic inhibition of GSNOR (Supporting Information). The chemical structures and relative potencies of N6022 and related compounds have been reported previously.[33−35] N6022 is a high-potency compound with an IC_{50} of approximately 8 nM in our GSNO reduction assay and 32 nM in

Table 1. Kinetic Constants of GSNOR for Different Substrate Pairs[a]

	GSNO	NADH	HMGSH	NAD^+
K_m (μM)	37 ± 0.6	37 ± 1.1	1.6 ± 0.3	6.6 ± 1.2
k_{cat} (min^{-1})	71 ± 1.2	70 ± 1.8	2.2 ± 0.10	2.3 ± 0.14
k_{cat}/K_m (M^{-1} s^{-1})	(1.9 ± 0.02) × 10^6	(1.9 ± 0.03) × 10^6	(1.4 ± 0.24) × 10^6	(3.5 ± 0.79) × 10^5

[a]Kinetic constants are the means and standard deviation determined at room temperature and pH 7.4 for the reaction of GSNO with NADH (n = 4) and pH 8.9 for the reaction of HMGSH with NAD^+ (n = 3).

dx.doi.org/10.1021/bi201785u | *Biochemistry* 2012, 51, 2157−2168

our HMGSH oxidation assay. Because of the high degree of conservation of amino acid sequence between ADH family members, the specificity of N6022 and related compounds for the GSNOR enzyme of the ADH family was investigated by measuring the relative potency of N6022 against three other human ADH enzymes: ADH IB, ADH II, and ADH IV (Figure 1).

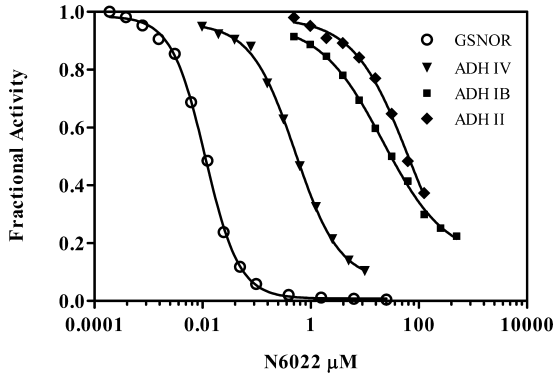

Figure 1. Inhibitor activity of N6022 against different classes of human ADH enzymes. GSNOR (ADH III) IC_{50} = 8 nM (GSNO substrate). ADH IV IC_{50} = 0.5 μM (hexanol substrate). AHD IB IC_{50} = 21 μM (ethanol substrate). ADH II IC_{50} = 67 μM (ethanol substrate).

On the basis of IC_{50} values, inhibition by N6022 is roughly 1000-fold more potent for GSNOR than for ADH IB and ADH II, and more than 50-fold more potent than for ADH IV. N6022 was also tested against human carbonyl reductase (hCBR1), an NADPH-dependent, short chain dehydrogenase, which has been shown to metabolize GSNO in vitro.[41] N6022 poorly inhibited hCBR1 activity with an IC_{50} of 221 μM, a value 4 orders of magnitude less potent than that for GSNOR (not shown). Several additional compounds related to N6022 that showed high potency for GSNOR were also tested against the other ADH enzymes. All compounds tested were found to be highly specific for GSNOR compared to the other ADH classes (Table 2).

Table 2. IC_{50} Values for GSNOR Inhibitor Compounds for Various ADH Enzymes[a]

inhibitor	ADH IB IC_{50} (μM)	ADH II IC_{50}[b] (μM)	ADH IV IC_{50} (μM)	GSNOR IC_{50}[c] (μM)
5a[d,e]	>250	ND	>1000	0.320
5f[e]	>500	ND	>500	0.210
N6022[e]	21	67	0.50	0.008
13c[e]	>500	68	291	0.057
13b[e]	>250	38	279	0.034
16[e]	>500	ND	>1000	0.044
8f[f]	>125	ND	0.571	0.008
5j[e]	>250	22	789	0.022

[a]The highest concentration of compound that could be tested was often limited by its solubility or by an interfering absorbance at 340 nm; in such instances, the value is presented as "greater than" the highest inhibitor concentration tested. [b]ND, not determined. Only a few compounds could be tested against ADH II because the enzyme precipitated and lost activity during storage. [c]GSNOR IC_{50} values differ slightly from those published elsewhere[33,35] because different data sets were used and assays were performed under slightly different formats. [d]Inhibitor **5b** was the initial lead compound identified by high-throughput screening. [e]From ref 33. [f]From ref 35.

N6022 Is a Tight-Binding, Fully Reversible Inhibitor. Our enzyme inhibitor screening assay was performed under steady state assumptions, which assume that the enzyme-bound inhibitor concentration ([EI]) is a small fraction of the free inhibitor concentration ([I]) used in the activity assay. This assumption is not true if the IC_{50} concentration approaches the enzyme concentration, and under such conditions, the inhibitor is considered a tight-binding inhibitor. Under our standard assay conditions, the enzyme concentration determined by absorbance was 12.6 nM (0.5 μg/mL), and the concentration of active enzyme determined experimentally was 11 nM (see Materials and Methods). Therefore, the IC_{50} of N6022 (8 nM) is close to the active GSNOR concentration (e.g., [EI] is not $\ll$ [I]), and N6022 is considered a tight-binding inhibitor. Under these conditions, steady state kinetic assumptions do not apply, and kinetic models for determining MOI were adjusted to account for the enzyme concentration.

Tight-binding inhibitors may also be slow binding; i.e., the equilibrium between the free and enzyme-bound inhibitor is established slowly, which requires special consideration in determining true enzyme affinity. The IC_{50} was measured with and without preincubation of the inhibitor and enzyme. No changes were seen after preincubation of N6022 with GSNOR for 0−30 min (not shown). Therefore, N6022 is not a slow-binding inhibitor. The order of addition of reagents also did not affect the reaction progress curve or IC_{50} value.

The reversibility of inhibition of GSNOR by N6022 was tested by measuring the recovery of enzyme activity after a large and rapid dilution of the enzyme−inhibitor complex. Enzyme at a concentration 100-fold above that required for an activity assay was incubated with inhibitor at 10-fold the IC_{50} and allowed to equilibrate. The mixture was then diluted 100-fold into reaction buffer containing substrate to initiate the reaction. The diluted mixture contained inhibitor at a concentration of one-tenth the IC_{50}, and therefore, the theoretical expected activity for a fully and rapidly reversible inhibitor under these conditions was 91%. The GSNOR activity relative to control (no inhibitor) was determined immediately after dilution (Figure 2). The recovered activity after dilution was 88.7 ± 2.5% (n = 3) of uninhibited activity, which was

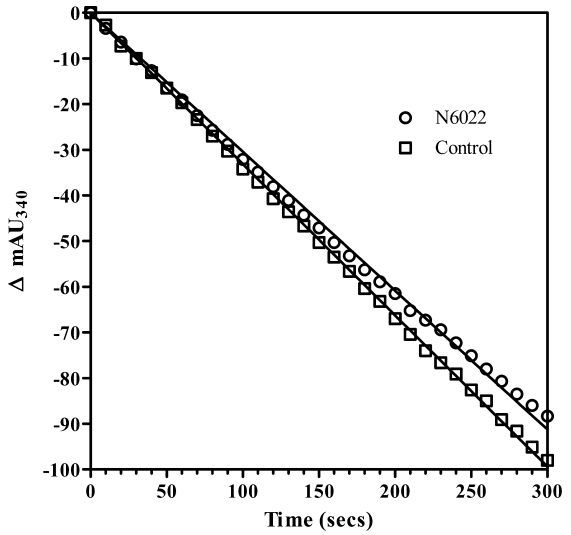

Figure 2. Reversibility of N6022 inhibitor activity. Example progress curves for the recovery of GSNOR activity after dilution are shown. The uninhibited control reaction is depicted with empty squares, and the reaction of the mixture preincubated with N6022 is depicted with empty circles. The progress curves have a negative slope, because they are monitoring the consumption of NADH (and to a lesser extent GSNO) by GSNOR.

dx.doi.org/10.1021/bi201785u | *Biochemistry* 2012, 51, 2157−2168

indistinguishable from the result of control assays in which N6022 at one-tenth the IC_{50} was measured directly with a recovery of 89.0 ± 3.6% (n = 3) of uninhibited activity. The rate of GSNOR activity remained linear over the 5 min measurement time. N6022 is a rapidly and fully reversible GSNOR inhibitor.

Mode of Inhibition. Once we established that N6022 was a tight-binding (but not a slow-binding), fully reversible inhibitor, we determined the kinetic MOI and calculated the various inhibitor dissociation constants (K_i) for both the reduction of GSNO by NADH and the oxidation of HMGSH by NAD^+. The K_i values for various steps in the reaction pathways (Scheme 1) were calculated using Cheng–Prusoff equations that provide a means of relating determinations of IC_{50} to K_i, provided one knows the MOI (i.e., competitive, noncompetitive, or uncompetitive), substrate concentration, and substrate K_m.[40] The equations and analysis we devised are detailed in Materials and Methods.

Because of the bisubstrate nature of the GSNOR reactions, we necessarily simplified our experimental analysis by holding one substrate at a constant, saturating concentration while that of the second substrate was varied. For the GSNO reduction reaction, the IC_{50} values for N6022 were determined over a range of GSNO concentrations while the NADH concentration was held constant. A plot of the IC_{50} values versus substrate concentration shows a decrease in IC_{50} as the substrate concentration increases, a characteristic of uncompetitive inhibition (Figure 3A). The data were fit to a Cheng–Prusoff model with a term for tight binding (eq 1, Materials and Methods) with a K_{i1} of 133 nM, a K_{i2} of 3.2 nM, and an α of 0.024. The same experiment was performed with variation of the NADH concentration while the concentration of GSNO was held constant. The IC_{50} value decreased with an increasing NADH concentration, and the MOI was purely uncompetitive with K_{i1} approaching infinity, K_{i2} equaling 1.4 nM, and α equaling 0 (Figure 3B).

The same analysis was performed for the HMGSH oxidation assay with NAD^+ as the cofactor. For the HMGSH substrate, the IC_{50} increased with an increasing substrate concentration, characteristic of a competitive inhibitor, until a plateau was reached at a high HMGSH concentration (Figure 3C). The plateau is likely the result of the reverse reduction reaction becoming sufficiently significant at high substrate concentrations to influence the overall absorbance signal. The MOI was mixed competitive with a K_{i1} of 2.8 nM, a K_{i2} of 12.8 nM, and an α of 4.6. For the NAD^+ cofactor, the mode of inhibition was mixed uncompetitive with a K_{i1} of 145 nM, a K_{i2} of 13.6 nM, and an α of 0.09 (Figure 3D). The results are summarized in Table 3.

K_i for N6022 and Other GSNOR Inhibitors. It is important to note that the K_{i1} or K_{i2} values from Table 3 do not represent the K_i of N6022 for free GSNOR, because one of the two cosubstrates was present at a saturating concentration

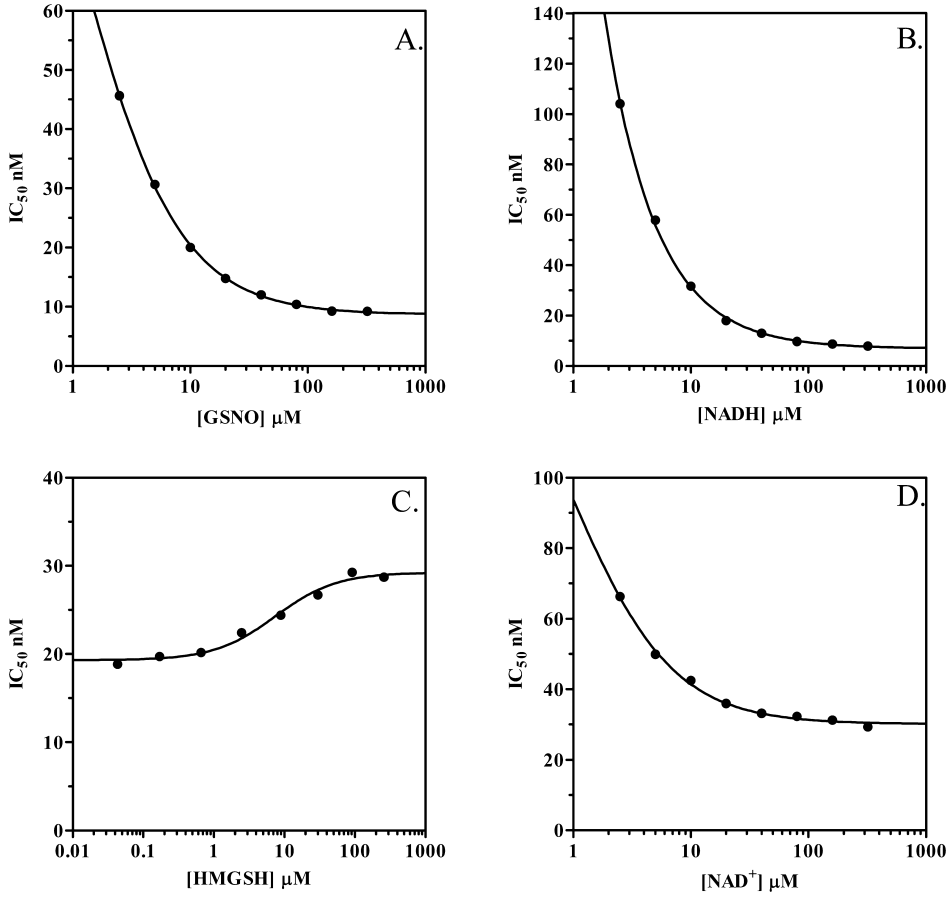

Figure 3. Mode of inhibition for N6022 against different substrates determined by measuring inhibitor IC_{50} as a function of substrate levels. The concentration of the varied substrate is given along the x-axis. (A and B) Reaction of GSNO with NADH. N6022 was mixed uncompetitive when the concentration of GSNO was varied and purely uncompetitive when the concentration of NADH was varied. (C and D) Reaction of HMGSH with NAD^+. N6022 was mixed competitive when the concentration of HMGSH was varied and mixed uncompetitive when the concentration of NAD^+ was varied.

dx.doi.org/10.1021/bi201785u | Biochemistry 2012, 51, 2157–2168

Table 3. N6022 Dissociation Constants and Modes of Inhibition Relative to a Varied Substrate[a]

varied substrate	constant substrate	K_{i1} (nM)	K_{i2} (nM)	α	MOI[b]
GSNO	NADH	133	3.2	0.024	mU
NADH	GSNO	∞	1.4	0	U
HMGSH	NAD^+	2.8	12.8	4.6	mC
NAD^+	HMGSH	145	13.6	0.09	mU

[a]The MOI relative to a varied substrate was determined by the value of α as defined in Materials and Methods. [b]Abbreviations: mU, mixed uncompetitive; U, uncompetitive; mC, mixed competitive.

in all the experiments. However, by incorporating the MOI results for each substrate considered separately, we were able to calculate the K_i of the N6022−GSNOR interaction. Equations 4 and 5 (Materials and Methods) were used to calculate the K_i of N6022 for GSNOR in the GSNO reduction assay and the K_i of N6022 for GSNOR in the HMGSH oxidation reaction, respectively. The second equation is similar to the first equation, except the enzyme concentration was 3 times higher for the HMGSH assay and the MOI for each substrate differed. For the GSNO reduction assay, the K_i for N6022 was 2.5 ± 0.2 nM (n = 2), and for the HMGSH oxidation reaction, the K_i for N6022 was 3.1 ± 0.5 nM (n = 2). The calculated K_i values are in good agreement between the GSNO and HMGSH reactions, despite the different reactions being studied and despite the different enzyme and substrate concentrations used for the two assays. Agreement in K_i values is to be expected for the two reactions, because we are calculating the dissociation constant of the inhibitor and free enzyme, and unlike the IC_{50} value, the K_i is not dependent on enzyme and substrate concentrations in the two assays.

The MOI analysis (IC_{50} as a function of substrate concentration) and K_i calculation were applied using the GSNOR-catalyzed reduction of GSNO by NADH for several other highly potent inhibitors (Table 4). All the inhibitors were fully reversible and best

Table 4. IC_{50} Values Compared to K_i Values for Different GSNOR Inhibitors[a]

inhibitor	IC_{50} (nM)	K_i (nM)
5a[b]	320	240
N6022[b]	8	2.5
13c[b]	57	42
13b[b]	34	21
16[b]	44	30
5w[d]	30	20
8f[c]	8	1.6
5j[b]	22	14

[a]K_i values were determined from the reaction of GSNO with NADH as described for N6022. The MOI for all inhibitors was either uncompetitive or mixed uncompetitive against GSNO and purely uncompetitive against NADH as defined by the experimentally determined α value. [b]From ref 33. [c]From ref 35. [d]From ref 49.

fit uncompetitive or mixed uncompetitive models against GSNO and were uncompetitive against NADH. The uncompetitive nature of these inhibitors toward GSNO meant that the IC_{50} value was approaching the K_i under our typical screening assay conditions (concentrations of substrate and cofactor greater than their K_m values), and generally, the IC_{50} value performed well as a measure of relative potency in our screening assay. For the most potent compounds, however, the relative potency by IC_{50} was limited by the enzyme concentration of the assay (i.e., N6022 and **8f**).

Dissociation of [^{14}C]N6022 Using Filter Binding Assays. Filter binding experiments using radiolabeled [^{14}C]N6022 were performed to measure directly the inhibitor dissociation constants of N6022 from the various enzyme species in an attempt to verify the results obtained from the kinetic studies. Unfortunately, the specific activity of [^{14}C]N6022 was not sufficiently high, and the K_i values were too low (low nanomolar range, per kinetic MOI studies) to perform most of the experiments successfully. We were, however, able to use the radiolabeled inhibitor to measure the ability of HMGSH to compete off [^{14}C]N6022 bound to the [^{14}C]N6022·GSNOR·NADH ternary complex and of GSNO to compete off [^{14}C]N6022 from the [^{14}C]N6022·GSNOR·NAD^+ complex (Figure 4). Substrates were

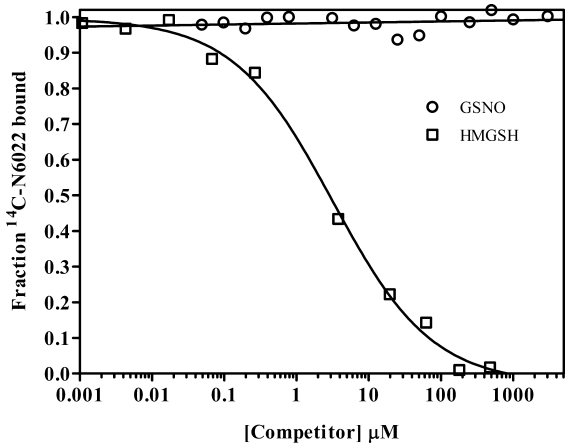

Figure 4. Substrate competition of GSNO and HMGSH for the [^{14}C]N6022·GSNOR·NAD^+ and [^{14}C]N6022·GSNOR·NADH ternary complexes, respectively.

tested against the complex containing the noncomplementary cofactor, because binding against the complementary cofactor complex would have resulted in catalysis. HMGSH, which forms the abortive ternary complex with NADH,[20,22] successfully competes off [^{14}C]N6022 from the [^{14}C]N6022·GSNOR·NADH complex with a calculated K_d of 400 nM for HMGSH and the GSNOR·NADH complex. GSNO, on the other hand, was unable to compete off the [^{14}C]N6022 from the [^{14}C]N6022·GSNOR·NAD^+ complex, even at very high GSNO concentrations, suggesting that GSNO is unable to form the abortive GSNO·GSNOR·NAD^+ complex. The inability of GSNO to form the abortive GSNO·GSNOR·NAD^+ ternary complex is an important observation that can explain why the MOI of N6022 is uncompetitive toward GSNO, even though GSNO and N6022 bind to the same site on the enzyme (see Discussion).

Structure of the N6022·GSNOR·NAD^+ Ternary Complex Compared to the HMGSH·GSNOR·NADH Ternary Complex. The structure of N6022 bound to the substrate binding pocket of the GSNOR·NAD^+ complex has been previously published[33] [Protein Data Bank (PDB) entry 3QJ5]. There is no structure of GSNO bound to GSNOR available, so we compared inhibitor binding in the N6022·GSNOR·NAD^+ ternary complex structure to substrate binding in the HMGSH·GSNOR·NADH ternary complex structure[20] (PDB entry 1MC5). A superimposition of these two structures shows a similar binding pose for N6022 and HMGSH in the GSNOR active site pocket [root-mean-square deviation of 0.43 Å (not shown)].

dx.doi.org/10.1021/bi201785u | Biochemistry 2012, 51, 2157−2168

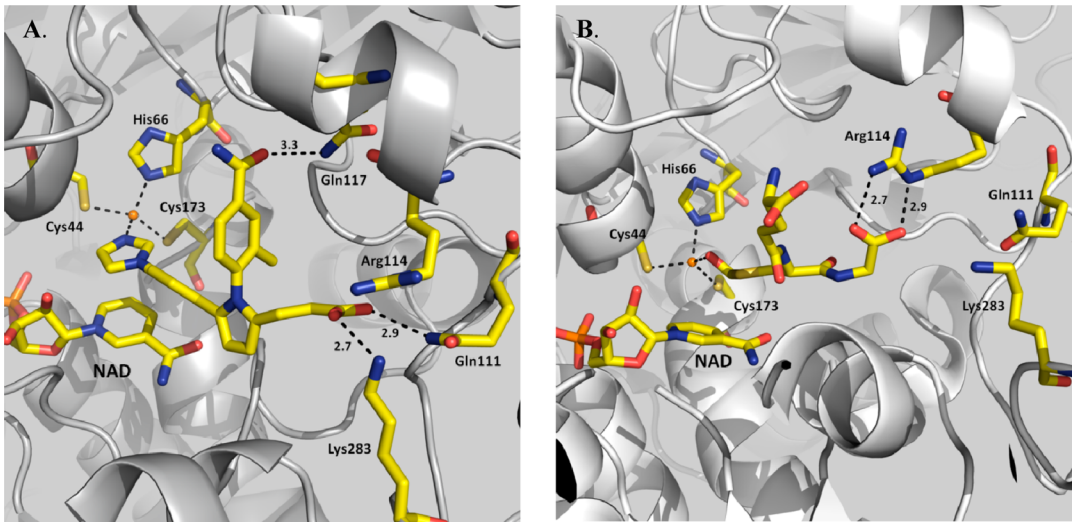

Figure 5. Comparison of N6022 and HMGSH binding within the GSNOR active site. (A) Interactions of N6022 with the GSNOR binding pocket in the N6022·GSNOR·NAD^+ ternary complex. (B) Interactions of HMGSH with the GSNOR binding pocket in the HMGSH·GSNOR·NADH ternary complex. Note that the viewing angle for the two images is not identical, and not all interactions are depicted. Bond distances represented by dashed lines are in angstroms.

The acid substituent of both compounds is oriented toward the anionic pocket, while the N6022 imidazole and HMGSH hydroxyl are directed toward the catalytic zinc where both compounds form part of the zinc coordination tetrahedron (Figure 5).

In the N6022 structure (Figure 5A), the propionic acid projects deeply into an anionic pocket within the GSNOR active site and engages in hydrogen bonding and salt bridge interactions with Gln111, Arg114, and Lys283 (from monomer B). Additional stabilization is provided by a hydrogen bond between the N6022 benzamide and Gln117 with additional water-mediated contacts. The central pyrrole moiety and adjacent hydrocarbon chains of N6022 make hydrophobic contacts with cleft residues Tyr92, Ile93, Met140, Val293, Ala317, and Val308/Thr309 (from monomer B). Finally, the alignment of N6022 along the substrate cleft orients the compound imidazole toward the catalytic zinc, and the imidazole nitrogen forms part of the active zinc coordination tetrahedron along with residues Cys44, His66, and Cys173. The imidazole ring is also stabilized through $\pi-\pi$ interactions with the nicatinamide ring of NAD^+. Generally, these inhibitor interactions with GSNOR resemble those observed for the HMGSH substrate (Figure 5B). HMGSH is tethered to the anionic pocket via the glycinyl carboxylate that interacts directly with Arg114 and indirectly with Glu111 via a water molecule. Additionally, the α-amino group from the γ-glutamate residue forms hydrogen bonds with Asp55 and Glu57. HMGSH also makes a number of hydrophobic interactions with the nonpolar residues that line the active site, and the hydroxyl group of HMGSH coordinates the active site zinc along with residues Cys44, His66, and Cys173. There were no discernible differences in the way the NAD^+ or NADH cofactor was bound in the two ternary structures compared here.

DISCUSSION

N6022 and related compounds were designed by structure–activity relationship to be potent and specific inhibitors of GSNOR, also known as the ADH Class III enzyme.[33−35] Members of the human ADH family of enzymes share up to 60% amino acid sequence identity, and roughly 80–90% homology, and overall, they share a very similar structure. However, they have a number of important differences in amino acids and structure that affect the substrate specificity and reaction mechanism. For example, the unbound ADH I enzymes have an "open" active site that necessitates an ordered reaction mechanism and requires cofactor binding prior to substrate binding. Binding of a cofactor to ADH I causes substantial domain movement and closure of the active site cleft allowing subsequent binding of small substrates such as ethanol (reviewed in ref 42). GSNOR, on the other hand, has a "semi-open" active site, and it undergoes only small structural changes upon binding either cofactor or substrate, thus allowing for larger substrates as well as a random order of addition of the substrate and cofactor.[19−22] The structure and mechanism of ADH IV more closely resemble those of ADH I than those of GSNOR with an ordered reaction mechanism and large domain closure.[43] The structure of human ADH II has not been reported, although a structure of the mouse homologue suggests an openness of the active site intermediate between ADH I and ADH III.[42] As a consequence of these structural differences, the different classes of ADH vary greatly in their substrate preferences, with ADH I and ADH II preferring small alcohols such as ethanol, ADH IV preferring retinol and hexanol, and GSNOR preferring the glutathione adducts GSNO and HMGSH. GSNOR does not oxidize ethanol to any significant degree. Therefore, given the substrate and mechanistic differences among the ADH family members, it might be expected that rational drug design efforts to maximize inhibitor interactions with the GSNOR substrate binding pocket could lead to novel compounds that do not bind well to other ADH family members. Nonetheless, it is important to screen for cross-reactivity with other enzyme family members to minimize possible off-target activities of any potential therapeutic compounds.

The inhibitory activity of N6022 and several related compounds was tested against human ADH IB, ADH II, and ADH IV. These compounds showed potent and specific inhibitor activity against GSNOR, with orders of magnitude less activity toward the other ADH enzymes as measured by IC_{50} for select substrates. Although they exhibit excellent specificity for GSNOR overall, some minor differences in specificity, particularly with regard to ADH IV, were noted. Compounds **5j**, **13b**, **13c**, and **16** showed less inhibitory

dx.doi.org/10.1021/bi201785u | *Biochemistry* 2012, 51, 2157–2168

activity toward ADH IV than N6022 (Table 2), but also less potency toward GSNOR, which is evident in their K_i values (Table 4). However, none of these compounds would be excluded as clinical candidates on the basis of either their specificity or potency as characterized so far. With N6022, for example, any inhibition of ADH IV should be minimal at the doses required to produce the optimal pharmacological effect observed in preclinical mouse models (C_{max} = 0.25 μg/mL[36]). Furthermore, the pharmacological consequences of any low-level, off-target inhibition of ADH IV are not expected to be significant. The physiological role of the enzyme, aside from its general alcohol detoxification properties and minor role in retinol metabolism, is not well understood, but ADH IV knockout mice were viable and fertile and displayed no obvious deficiencies, except if exposed to severe gestational vitamin A deficiency.[44]

In addition to testing the specificity of our GSNOR inhibitors against other human ADH isozymes, we studied the basic biochemical mechanism of inhibition. The crystal structure of the N6022·GSNOR·NAD^+ complex shows the inhibitor bound in the substrate binding pocket like a competitive inhibitor.[33] Comparison of the N6022·GSNOR·NAD^+ structure with the HMGSH·GSNOR·NADH structure reveals that the inhibitor engages in active site interactions generally similar to those of the substrate HMGSH. The acid component of both compounds interacts with the anionic pocket of the active site; the central regions of the compounds participate in hydrophobic interactions with a number of residues lining the binding cleft; and both HMGSH and N6022 form part of the active site zinc coordination tetrahedron. The GSNOR inhibitors presented here have been optimized to fit the volume of the binding pocket even better than substrate, and the additional contacts made by these compounds can account for their high potency and specific affinity. None of the inhibitors presented here participate in any covalent interactions with the enzyme, and none are substrates or show mechanism-based inhibition of GSNOR. Dilution and recovery experiments confirmed that the inhibitors were fully and rapidly reversible. Several of the inhibitors, in particular N6022, were considered tight-binding because their IC_{50} concentrations approached the enzyme concentration of the assay. The inhibitors were not slow-binding. With this information, we developed a strategy to characterize the kinetic mode of inhibition and to calculate the K_i of the inhibitors based on the Cheng–Prussoff approach.[40]

Using the Cheng–Prusoff approach, along with modifications described by Copeland, we determined the kinetic MOI so that we could calculate the K_i of the inhibitor–GSNOR interaction for several of our more potent inhibitors. Unlike the IC_{50}, the K_i is independent of the enzyme, substrate, and cofactor concentrations, and the K_i value is not limited by the tight-binding nature of our inhibitors. We accounted for the bisubstrate nature of GSNOR, as well as the tight-binding nature of the inhibitor in our equations. This approach could be used to evaluate the inhibitor mechanism for other bisubstrate enzyme reactions. Determining the K_i allowed us to distinguish differences in our high-potency compounds that were not apparent in the IC_{50} values, thus aiding our rational drug design program and lead optimization. For example, N6022 and compound **8f** had K_i values in the low nanomolar range. The high potency of these two compounds can be explained because they both contain an imidazole group that, based on X-ray crystallography data, makes an additional contact with the catalytic zinc of GSNOR and, if a cofactor is also bound, forms a π–π interaction with the nicatinamide ring.[33,35]

Surprisingly, despite the competitive-like binding of our inhibitors in the substrate binding pocket, the GSNOR inhibitors studied here behaved operationally like uncompetitive inhibitors against the GSNO substrate in the kinetic MOI assays. Increasing the GSNO concentration in the GSNO reduction reaction did not overcome inhibition but improved apparent potency based on the IC_{50} value, a defining characteristic of uncompetitive inhibition.[38,45] The inhibitors behaved with the expected competitive MOI against the HMGSH substrate in the oxidation assay. A similar phenomenon was also observed for the lower-potency inhibitors reported by others, which behaved like noncompetitive inhibitors (same as mixed uncompetitive by our definitions) in the GSNO reduction assay.[25,32]

These pieces of data present a conundrum. On one hand, crystallography data clearly show N6022 and related compounds bound in the substrate binding pocket, in a way that excludes substrate and in a manner classically considered competitive inhibition.[33] On the other hand, the kinetic analysis following established Cheng–Prusoff definitions categorizes inhibition against the GSNO substrate as uncompetitive, although the inhibition against the HMGSH substrate showed the expected competitive MOI. Although the structure of GSNO bound to GSNOR has not been reported, it is readily assumed to bind to the substrate binding pocket in a manner analogous to that of HMGSH. Docking simulations of GSNO bound in the substrate binding site have been published.[25] GSNO and HMGSH are glutathione adducts identical except for the functional group attached to the sulfur atom (see the Supporting Information).

We propose a model for resolving this conundrum and explain the uncompetitive MOI toward the GSNO substrate, based on our observation that GSNO was not able to displace the radiolabeled inhibitor from the [^{14}C]N6022·GSNOR·NAD^+ ternary complex. We concluded that GSNO was unable to bind to the GSNOR·NAD^+ complex and form a stable abortive GSNO·GSNOR·NAD^+ structure. Further evidence, albeit circumstantial, supporting this conclusion comes from our inability to obtain crystals of the abortive GSNO·GSNOR·NAD^+ ternary complex despite repeated attempts (not published). The HMGSH·GSNOR·NADH abortive structure, on the other hand, forms readily, and a crystal structure has been published.[20]

Scheme 2 illustrates our model of how GSNOR inhibitors could appear uncompetitive toward the GSNO substrate in the GSNO reduction reaction, despite the fact that they displace GSNO from the substrate binding pocket like a traditionally competitive inhibitor. In our closed assay system, the starting components are only GSNOR, NADH, GSNO, and the inhibitor. The GSNO used in these studies is a highly purified,

Scheme 2. Illustration of the Reaction Pathway for the Reduction of GSNO by GSNOR in a Closed Assay System[a]

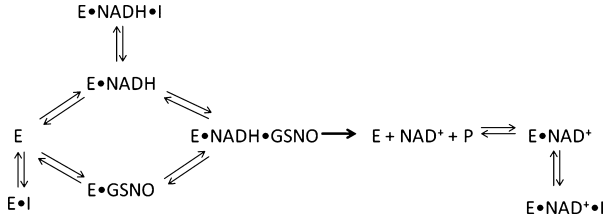

[a]Abbreviations: E, GSNOR; I, inhibitor; P, product. The reaction is assumed to be random order,[22] and either GSNO or NADH can bind the enzyme first. The inhibitor can bind to the free enzyme or to either enzyme·cofactor binary complex. GSNO cannot bind to the enzyme·NAD^+ species and so does not "compete" with the inhibitor for that enzyme species.

dx.doi.org/10.1021/bi201785u | Biochemistry 2012, 51, 2157–2168

pharmaceutical grade material and not contaminated with GSH, so there is no free GSH in our assay to interact with product or substrate. As soon as the reaction is initiated, even in the presence of inhibitor, some of the GSNOR catalyzes the reduction of GSNO, and some NAD^+ is produced. Glutathione sulfinamide product is also produced, but it is already established that it is neither an inhibitor nor a substrate for GSNOR.[23] In our scheme, GSNO can bind free GSNOR, or the GSNOR·NADH complex, but cannot bind the GSNOR·NAD^+ complex. On the other hand, the inhibitor can bind to all three complexes. At higher starting GSNO concentrations, more NAD^+ will be produced at the initiation of the reaction (high concentrations of GSNO displace the lower concentrations of the inhibitor initially), and there will be more GSNOR·NAD^+ complex early in the reaction than at lower concentrations of GSNO. Almost immediately, however, the inhibitor will now bind more enzyme species than GSNO. The overall result is that the inhibitor behaves with an uncompetitive MOI and has a lower IC_{50} (higher relative potency) at high GSNO concentrations because more NAD^+ will be present. HMGSH shows the more expected competitive MOI in the kinetic experiments (IC_{50} increases as the HMGSH concentration increases) because, like inhibitor, it can bind free enzyme and either the GSNOR·NAD^+ or GSNOR·NADH binary complexes, and HMGSH displaces the inhibitor from all complexes. The MOI result for the HMGSH oxidation reaction was determined as mixed competitive rather than purely competitive in our experiments because the reversible nature of the reaction, as well as product inhibition, can contribute significantly to the absorbance signal at higher substrate concentrations. The filter binding experiment with a radiolabeled inhibitor, however, demonstrated that HMGSH can fully displace the inhibitor from the [^{14}C]N6022·GSNOR·NADH complex in a truly competitive manner. The fact that an inhibitor can have two different mechanisms for two different substrates that bind the same active site on an enzyme is a reminder that conclusions about the location of inhibitor binding relative to substrate cannot be drawn from MOI studies relating K_i to IC_{50} alone, nor do structural data give a definitive picture of the kinetic inhibitor mechanism in the absence of biochemical data.

We have considered alternative situations that might explain how our GSNOR inhibitors could have an uncompetitive MOI against the GSNO reaction despite binding in the substrate binding pocket. We considered whether high concentrations of GSNO could modify (i.e., either by nitrosation or glutathionation) the enzyme and decrease the activity. However, preincubation of GSNO with GSNOR did not have any effect on enzyme activity (not shown). Another possible explanation would be that GSNO and N6022 bind simultaneously to GSNOR. However, this explanation seems unlikely as both compounds are known to bind the substrate active site, the active site is not sufficiently large to accommodate both molecules at once, and there is no known alternative binding site on the enzyme that would allow for allosteric inhibition by N6022. Therefore, with the data so far available, Scheme 2 provides the best way to resolve the kinetic and structural data.

Our model requires that the oxidation state of the cofactor strongly influences GSNO binding. A high-resolution structure of GSNO bound to GSNOR, so far elusive, would provide valuable information to address this question. We do know that the oxidation state of the cofactor substantially affects the dissociation constant of the cofactor for GSNOR; the reduced cofactor binds with an affinity roughly 250 times greater than that of the oxidized cofactor (K_d = 0.043 μM for NADH; K_d = 11.5 μM for NAD^+).[22] An explanation for this large difference in binding affinity has not been determined. Additionally, despite the high degree of similarity between the HMGSH and GSNO substrates, they must have significant differences in how they interact with the catalytic site on the enzyme and how the proton relay is performed for the two opposite oxidoreduction reactions. Much remains to be learned to understand the catalytic details of reduction of GSNO by GSNOR.

The inhibitor mechanism has important effects on the pharmacological properties of a drug and can even determine the clinical success or failure of a particular compound.[46,47] Beyond being a valuable exercise for ranking relative inhibitor potency and aiding lead optimization, what implications might the MOI studies presented here have for the pharmacological properties of N6022 and this class of GSNOR inhibitors? Of particular interest for these compounds is whether they will behave as competitive or uncompetitive inhibitors in vivo. The pharmacological disadvantage of purely competitive enzyme inhibitors as drugs is that accumulation of the substrate following inhibition may overcome the inhibition, leading to larger doses of drug needed to sustain the desired level of inhibition.[47,48] Although the GSNOR inhibitors discussed here at first appear competitive because structural data show they bind in the substrate pocket, increasing the GSNO concentration does not overcome inhibition but rather enhances it in our assay system. Our data suggest that the uncompetitive mechanism may translate pharmacologically for the GSNO substrate and that GSNO accumulation in vivo will not overcome inhibition of the GSNO reduction reaction, because our inhibitors bind with very high affinity to more GSNOR species than does the GSNO substrate. However the in vivo scenario remains very complicated, and the degree of GSNOR inhibition, and subsequent GSNO accumulation, will depend on the enzyme and GSNO concentrations, the concentration and oxidation state of the cofactor, and the presence of any competing substrates such as HMGSH.

In conclusion, we have identified reversible, highly potent, specific inhibitors of GSNOR for therapeutic use in cases where GSNO homeostasis has been disrupted. Nonoptimized inhibitors of GSNOR have been reported previously,[25,32] but N6022 and the other compounds mentioned here are 100–1000-fold more potent than those structures and are more able to distinguish specificity between ADH family members. The GSNOR inhibitors described here were also shown to be specific when screened against a broad panel of human receptors commonly used in preliminary safety screens of potential drug candidates.[33−35] These are the first GSNOR inhibitors of suitable potency and specificity for pharmacological development. Several compounds have already shown tolerability and efficacy in preclinical animal models, and N6022 is currently in early phase clinical studies in humans.

■ ASSOCIATED CONTENT

Supporting Information

A figure comparing the GSNO reduction and HMGSH oxidation reactions performed by GSNOR, as well as the chemical structure of inhibitor N6022. This material is available free of charge via the Internet at http://pubs.acs.org.

AUTHOR INFORMATION

Corresponding Author

*N30 Pharmaceuticals, LLC, 3122 Sterling Circle, Suite 200, Boulder, CO 80301. E-mail: Jane.richards@n30pharma.com. Phone: (720) 945-7733. Fax: (303) 440-8399.

Notes

The authors declare no competing financial interest.

ACKNOWLEDGMENTS

We thank Adam Stout for help preparing the Supporting Information and Sarah Mutka for critical review of the manuscript.

ABBREVIATIONS

ADH, alcohol dehydrogenase; FDH, formaldehyde dehydrogenase; GSH, glutathione; GSNO, *S*-nitrosoglutathione; GSNOR, *S*-nitrosoglutathione reductase; GSSG, glutathione disulfide; HMGSH, *S*-hydroxymethylglutathione; MOI, mode of inhibition; NAD^+ and NADH, nicotinamide adenine dinucleotide; NO, nitric oxide.

REFERENCES

(1) Wagner, F. W., Parés, X., Holmquist, B., and Vallee, B. L. (1984) Physical and enzymatic properties of a class III isozyme of human liver alcohol dehydrogenase: χ-ADH. *Biochemistry 23*, 2193−2199.

(2) Juliá, P., Boleda, M. D., Farrés, J., and Parés, X. (1987) Mammalian alcohol dehydrogenase: Characteristics of class III isoenzymes. *Alcohol* No. Suppl. 1, 169−173.

(3) Koivusalo, M., Baumann, M., and Uotila, L. (1989) Evidence for the identity of glutathione-dependent formaldehyde dehydrogenase and class III alcohol dehydrogenase. *FEBS Lett. 257*, 105−109.

(4) Holmquist, B., and Vallee, B. L. (1991) Human liver class III alcohol and glutathione dependent formaldehyde dehydrogenase are the same enzyme. *Biochem. Biophys. Res. Commun. 178*, 1371−1377.

(5) Staab, C. A., Hellgren, M., and Höög, J. O. (2008) Dual functions of alcohol dehydrogenase 3: Implications with focus on formaldehyde dehydrogenase and S-nitrosoglutathione reductase activities. *Cell. Mol. Life Sci. 65*, 3950−3960.

(6) Danielsson, O., and Jörnvall, H. (1992) "Enzymogenesis": Classical liver alcohol dehydrogenase origin from the glutathione-dependent formaldehyde dehydrogenase line. *Proc. Natl. Acad. Sci. U.S.A. 89*, 9247−9251.

(7) Höög, J. O., Hedberg, J. J., Strömberg, P., and Svensson, S. (2001) Mammalian alcohol dehydrogenase: Functional and structural implications. *J. Biomed. Sci. 8*, 71−76.

(8) Gonzàlez-Duarte, R., and Albalat, R. (2005) Merging protein, gene and genomic data: The evolution of the MDR-ADH family. *Heredity 95*, 184−197.

(9) Estonius, M., Danielsson, O., Karlsson, C., Persson, H., Jörnvall, H., and Höög, J. O. (1993) Distribution of alcohol and sorbitol dehydrogenases. Assessment of mRNA species in mammalian tissues. *Eur. J. Biochem. 215*, 497−503.

(10) Estonius, M., Svensson, S., and Höög, J. O. (1996) Alcohol dehydrogenase in human tissues: Localisation of transcripts coding for five classes of the enzyme. *FEBS Lett. 397*, 338−342.

(11) Nishimura, M., and Naito, S. (2006) Tissue-specific mRNA expression profiles of human phase I metabolizing enzymes except for cytochrome P450 and phase II metabolizing enzymes. *Drug Metab. Pharmacokinet. 21*, 357−374.

(12) Keller, D. A., Heck, H. D., Randall, H. W., and Morgan, K. T. (1990) Histochemical localization of formaldehyde dehydrogenase in the rat. *Toxicol. Appl. Pharmacol. 106*, 311−326.

(13) Jensen, D. E., Belka, G. K., and Du Bois, G. C. (1998) S-Nitrosoglutathione is a substrate for rat alcohol dehydrogenase class III isoenzyme. *Biochem. J. 331*, 659−668.

(14) Liu, L., Hausladen, A., Zeng, M., Que, L., Heitman, J., and Stamler, J. S. (2001) A metabolic enzyme for S-nitrosothiol conserved from bacteria to humans. *Nature 410*, 490−494.

(15) Foster, M. W., McMahon, T. J., and Stamler, J. S. (2003) S-nitrosylation in health and disease. *Trends Mol. Med. 9*, 160−168.

(16) Foster, M. W., Hess, D. T., and Stamler, J. S. (2009) Protein S-nitrosylation in health and disease: A current perspective. *Trends Mol. Med. 9*, 391−404.

(17) Lima, B., Forrester, M. T., Hess, D. T., and Stamler, J. S. (2010) S-nitrosylation in cardiovascular signaling. *Circ. Res. 106*, 633−646.

(18) Yang, Z. N., Bosron, W. F., and Hurley, T. D. (1997) Structure of human chi chi alcohol dehydrogenase: A glutathione-dependent formaldehyde dehydrogenase. *J. Mol. Biol. 265*, 330−343.

(19) Sanghani, P. C., Robinson, H., Bosron, W. F., and Hurley, T. D. (2002) Human glutathione-dependent formaldehyde dehydrogenase. Structures of apo, binary, and inhibitory ternary complexes. *Biochemistry 41*, 10778−10786.

(20) Sanghani, P. C., Bosron, W. F., and Hurley, T. D. (2002) Human glutathione-dependent formaldehyde dehydrogenase. Structural changes associated with ternary complex formation. *Biochemistry 41*, 15189−15194.

(21) Sanghani, P. C., Robinson, H., Bennett-Lovsey, R., Hurley, T. D., and Bosron, W. F. (2003) Structure-function relationships in human Class III alcohol dehydrogenase (formaldehyde dehydrogenase). *Chem.-Biol. Interact. 143−144*, 195−200.

(22) Sanghani, P. C., Stone, C. L., Ray, B. D., Pindel, E. V., Hurley, T. D., and Bosron, W. F. (2000) Kinetic mechanism of human glutathione-dependent formaldehyde dehydrogenase. *Biochemistry 39*, 10720−10729.

(23) Hedberg, J. J., Griffiths, W. J., Nilsson, S. J., and Höög, J. O. (2003) Reduction of S-nitrosoglutathione by human alcohol dehydrogenase 3 is an irreversible reaction as analysed by electrospray mass spectrometry. *Eur. J. Biochem. 270*, 1249−1256.

(24) Staab, C. A., Ålander, J., Morgenstern, R., Grafström, R. C., and Höög, J. O. (2009) The Janus face of alcohol dehydrogenase 3. *Chem.-Biol. Interact. 178*, 29−35.

(25) Staab, C. A., Hellgren, M., Grafström, R. C., and Höög, J. O. (2009) Medium-chain fatty acids and glutathione derivatives as inhibitors of S-nitrosoglutathione reduction mediated by alcohol dehydrogenase 3. *Chem.-Biol. Interact. 180*, 113−118.

(26) Staab, C. A., Ålander, J., Brandt, M., Lengqvist, J., Morgenstern, R., Grafström, R. C., and Höög, J. O. (2008) Reduction of S-nitrosoglutathione by alcohol dehydrogenase 3 is facilitated by substrate alcohols via direct cofactor recycling and leads to GSH-controlled formation of glutathione transferase inhibitors. *Biochem. J. 413*, 493−504.

(27) Que, L. G., Liu, L., Yan, Y., Whitehead, G. S., Gavett, S. H., Schwartz, D. A., and Stamler, J. S. (2005) Protection from experimental asthma by an endogenous bronchodilator. *Science 308*, 1618−1621.

(28) Que, L. G., Yang, Z., Stamler, J. S., Lugogo, N. L., and Kraft, M. (2009) S-Nitrosoglutathione reductase: An important regulator in human asthma. *Am. J. Respir. Crit. Care Med. 180*, 226−231.

(29) Gaston, B., Reilly, J., Drazen, J. M., Fackler, J., Ramdev, P., Arnelle, D., Mullins, M. E., Sugarbaker, D. J., Chee, C., and Singel, D. J. (1993) Endogenous nitrogen oxides and bronchodilator S-nitrosothiols in human airways. *Proc. Natl. Acad. Sci. U.S.A. 90*, 10957−10961.

(30) Fortenberry, J. D., Owens, M. L., and Brown, L. A. (1999) S-Nitrosoglutathione enhances neutrophil DNA fragmentation and cell death. *Am. J. Physiol. 276*, L435−L442.

(31) Reynaert, N. L., Ckless, K., Korn, S. H., Vos, N., Guala, A. S., Wouters, E. F., van der Vliet, A., and Janssen-Heininger, Y. M. (2004) Nitric oxide represses inhibitory κB kinase through S-nitrosylation. *Proc. Natl. Acad. Sci. U.S.A. 101*, 8945−8950.

(32) Sanghani, P. C., Davis, W. I., Fears, S. L., Green, S. L., Zhai, L., Tang, Y., Martin, E., Bryan, N. S., and Sanghani, S. P. (2009) Kinetic and cellular characterization of novel inhibitors of S-nitrosoglutathione reductase. *J. Biol. Chem. 284*, 24354−24362.

(33) Sun, X., Wasley, J. W., Qiu, J., Blonder, J. P., Stout, A. M., Green, L. S., Strong, S. A., Colagiovanni, D. B., Richards, J. P., Mutka, S. C., Chun, L., and Rosenthal, G. J. (2011) Discovery of S-nitrosoglutathione reductase inhibitors: Potential agents for the treatment of asthma and other inflammatory diseases. *ACS Med. Chem. Lett. 2*, 5849−5853.
(34) Sun, X., Qiu, J., Strong, S. A., Green, L. S., Wasley, J. W., Colagiovanni, D. B., Mutka, S. C., Blonder, J. P., Stout, A. M., Richards, J. P., Chun, L., and Rosenthal, G. J. (2011) Structure-activity relationships of pyrrole based S-nitrosoglutathione reductase inhibitors: Pyrrole regioisomers and propionic acid replacement. *Bioorg. Med. Chem. Lett. 21*, 3671−3675.
(35) Sun, X., Qiu, J., Strong, S. A., Green, L. S., Wasley, J. W., Blonder, J. P., Colagiovanni, D. B., Mutka, S. C., Stout, A. M., Richards, J. P., and Rosenthal, G. J. (2011) Discovery of potent and novel S-nitrosoglutathione reductase inhibitors devoid of cytochrome P450 activities. *Bioorg. Med. Chem. Lett. 21*, 5849−5853.
(36) Colagiovanni, D. B., Drolet, D. W., Langlois-Forget, E., Piché, M. P., Looker, D., and Rosenthal, G. J. (2012) A nonclinical safety and pharmacokinetic evaluation of N6022: A first-in-class S-nitrosoglutathione reductase inhibitor for the treatment of asthma. *Regul. Toxicol. Pharmacol. 62*, 115−124.
(37) Copeland, R. A. (2005) Tight Binding Inhibition. In *Evalulation of Enzyme Inhibitors in Drug Discovery*, pp 178−213, John Wiley & Sons Inc., Hoboken, NJ.
(38) Copeland, R. A. (2005) Reversible Modes of Inhibitor Interactions with Enzymes. In *Evaluation of Enzyme Inhibitors in Drug Discovery*, pp 48−81, John Wiley & Sons, Inc., Hoboken, NJ.
(39) Copeland, R. A. (2000) Determinig the K_i for tight binding inhibitors. In *Enzymes: A Practical Introduction to Structure, Mechanism and Data Analysis*, 2nd ed., pp 310−313, Wiley-VCH, Inc., New York.
(40) Cheng, Y., and Prusoff, W. H. (1973) Relationship between the inhibition constant (K_I) and the concentration of inhibitor which causes 50% inhibition (I_{50}) of an enzymatic reaction. *Biochem. Pharmacol. 22*, 3099−3108.
(41) Bateman, R. L., Rauh, D., Tavshanjian, B., and Shokat, K. M. (2008) Human carbonyl reductase 1 is an S-nitrosoglutathione reductase. *J. Biol. Chem. 283*, 35756−35762.
(42) Eklund, H., and Ramaswamy, S. (2008) Medium- and short-chain dehydrogenase/reductase gene and protein families: Three-dimensional structures of MDR alcohol dehydrogenases. *Cell. Mol. Life Sci. 65*, 3907−3917.
(43) Xie, P., Parsons, S. H., Speckhard, D. C., Bosron, W. F., and Hurley, T. D. (1997) X-ray structure of human class IV sigma sigma alcohol dehydrogenase. Structural basis for substrate specificity. *J. Biol. Chem. 272*, 18558−18563.
(44) Deltour, L., Foglio, M. H., and Duester, G. (1999) Impaired retinol utilization in Adh4 alcohol dehydrogenase mutant mice. *Dev. Genet. 25*, 1−10.
(45) Copeland, R. A. (2005) Lead Optimization and Structure-Activity Relationships for Reversible Inhibitors. In *Evalation of Enzyme Inhibitors in Drug Discovery*, pp 111−140, John Wiley & Sons, Inc., Hoboken, NJ.
(46) Swinney, D. C. (2004) Biochemical mechanisms of drug action: What does it take for success? *Nat. Rev. Drug Discovery 3*, 801−808.
(47) Swinney, D. C. (2009) The role of binding kinetics in therapeutically useful drug action. *Curr. Opin. Drug Discovery Dev. 12*, 31−39.
(48) Westley, A. M., and Westley, J. (1996) Enzyme inhibition in open systems. Superiority of uncompetitive agents. *J. Biol. Chem. 271*, 5347−5352.
(49) Sun, X., Qiu, J., Strong, S. A., Green, L. S., Wasley, J. W., Blonder, J. P., Colagiovanni, D. B., Stout, A. M., Mutka, S. C., Richards, J. P., and Rosenthal, G. J. (2012) Structure-activity relationship of pyrrole based S-nitrosoglutathione reductase inhibitors: Carboxamide modification. *Bioorg. Med. Chem. Lett.*, DOI: 10.1016/j.bmcl.2012.01.047.